

See discussions, stats, and author profiles for this publication at: <https://www.researchgate.net/publication/319414574>

Magnetoresistance of graphite intercalated with cobalt

Article in *Journal of Materials Science* · August 2017

DOI: 10.1007/s10853-017-1511-x

CITATIONS

0

READS

47

8 authors, including:



Igor B Berkutov

North Carolina State University

54 PUBLICATIONS 206 CITATIONS

[SEE PROFILE](#)



Yuriy Prylutsky

National Taras Shevchenko University of Kyiv

270 PUBLICATIONS 2,175 CITATIONS

[SEE PROFILE](#)



Uwe Ritter

Technische Universität Ilmenau

222 PUBLICATIONS 2,076 CITATIONS

[SEE PROFILE](#)

Some of the authors of this publication are also working on these related projects:




'Configuration and size effects in electronic transport of doped graphene' (2015–2017) [View project](#)



Electronics of Fullerene Nanoscale Morphologies in Hybrid Solar Cells [View project](#)



Magnetoresistance of graphite intercalated with cobalt

Iryna Ovsienko¹, Lyudmila Matzui¹, Igor Berkutov², Il'gar Mirzoiev³, Tetyana Len¹, Yuriy Prylutsky¹, Oleksandr Prokopov¹, and Uwe Ritter^{4,*} 

¹Taras Shevchenko National University of Kyiv, Volodymyrska Str., 64, Kiev 01601, Ukraine

²Department of Physics, North Carolina State University, Raleigh, NC 27695, USA

³Verkin Institute for Low Temperature Physics and Engineering, NAS of Ukraine, Nauky Ave. 47, Kharkiv 61103, Ukraine

⁴Technical University of Ilmenau, 25 Weimarer Str, 98693 Ilmenau, Germany

Received: 22 May 2017

Accepted: 22 August 2017

Published online:
31 August 2017

© Springer Science+Business
Media, LLC 2017

ABSTRACT

The results of experimental studies of magnetoresistance, resistivity and Hall coefficient of graphite intercalated with cobalt are presented. A highly oriented pyrolytic graphite was chosen as source for intercalation. A two-step method of synthesis was used for graphite intercalation compound (GIC) obtaining. The electro- and magnetoresistance and Hall coefficient were measured in temperature range of (1.6–293) K and magnetic field up to 5 T. The effects of asymmetric and linear relatively to magnetic field magnetoresistance have been revealed for GIC. It was shown that the linear magnetoresistance is not saturated with increasing magnetic field up to 5 T and is not dependent on temperature. The effect of linear magnetoresistance in GIC was explained within Abrikosov model of quantum magnetoresistance.

Introduction

It is known that for metals and semiconductors with closed Fermi surface the resistance in a weak magnetic field depends quadratically on it, and with increasing magnetic field the resistance reaches saturation. Exceptions are materials with an open Fermi surface or compensated homogeneous semiconductors. In such materials the resistance increases with increasing magnetic field proportionally to square of it but without saturation. However, the nonsaturating and linear magnetoresistance has been revealed for a number of narrow-gap materials, such as thin films of doped silver chalcogenides [1–3], epitaxial layers InSb [4], disordered

semiconductors MnAs-GaAs [5], and also for layered structure PrFeAsO [6]. Linear magnetoresistance has been revealed in topological insulator thin films [7–9] too. Now there are two approaches for theoretical explanation of the magnetoresistance effect. The first approach is purely classical, and it is based on the importance of the phase inhomogeneities of nanometers scale [1]. This approach is applicable at moderate temperatures and only for the systems, where a mean size or some characteristic size of inhomogeneities $l_c \gg l_0$ (l_0 is a free path length of the charge carriers). In the framework of such approach Parish and Littlewood proposed the resistor network model that mimics inhomogeneous conducting media. This model was extended to the

Address correspondence to E-mail: uwe.ritter@tu-ilmenau.de

case of three-dimensional systems [10]. In this classical model, the linear dependence of the resistance on magnetic field is linked in a simple manner to electrical disorder. Other quantum approach to explain the linear magnetoresistance was proposed by Abrikosov. This approach is based on the quantum theory of possible changes of spectrum properties of semimetals or narrow-gap semiconductors [11]. It can be applied, for example, for an explanation of low-temperature properties of $\text{Ag}_{2+\delta}\text{Te}$ [2]. The necessary conditions for the manifestation of quantum linear magnetoresistance effect in the materials according to the Abrikosov mechanism are following: an approximately linear energy spectrum, carriers of very low effective mass, and an approximately zero band gap. Moreover, these materials subjected to a magnetic field should reach the quantum limit, where all electrons occupy the lowest Landau level.

One of the most promising materials for studying quantum linear magnetoresistance effect is graphene because of its unusual band structure with naturally zero band gap and a linear dispersion. Indeed, there are many articles, in which quantum linear magnetoresistance effect is observed in multilayer epitaxial graphene [12, 13], in the disordered graphene layers [14, 15] and even in the fine crystalline bulk graphite [16]. Another promising material for the study of quantum linear magnetoresistance could be graphite intercalation compounds (GICs). GICs are formed, when monoatomic or monomolecular layers of alkali metals, alkali earth metals, rare-earth elements, acids and salts are introduced in the interlayer space of graphite [17]. The peculiarity of intercalation process is a charge transfer from intercalate molecules to graphite layers resulting in graphite layers enriched with additional charge carriers. GIC of low stages (stage is the number of graphite layers between two successive intercalates layers) has the linear (for first-stage compounds) or quasi-linear (for second-stage compounds) dispersion law, a zero band gap, a weak interaction between graphite and intercalate layers. The only thing, that can hinder the observation of the quantum effect, is the significant increase in the carrier's effective mass in the process of intercalation. However, there are intercalation compounds for which the increase in carrier's effective mass is the minimum, for example, the GICs with transition metals [18, 19]. Properties of GICs with transition

metal are significantly different from those of traditional GICs (for example, GICs with metal chlorides). For acceptor GICs with metal chlorides a significant redistribution of charge between the graphite layers and intercalate layers is observed, whereas in the GICs with transition metals the charge redistribution is insignificant or completely absent. Thus, the research of GICs with transition metals is interesting to reveal a linear magnetoresistance effect in them.

It should be noted that extended surface of nano-size building blocks based on carbon is their peculiarity influencing the system properties as a whole. So, the developed surface area of single-walled carbon nanotubes (SWCNTs) impacts on the properties of liquid systems with their adding by changing the thermodynamic parameters [20–22]. Moreover, there is a possibility of enhancing SWCNT bioactivity by functionalization with carboxyl groups [23–25]. It motivates the usage of graphene-like compounds in combination with various dopants/intercalates/adatoms [26–28].

Thus, the aim of this work is to synthesize and study in detail the temperature and magnetic field dependences of magnetoresistance of graphite intercalated with cobalt as a new promising material for applied technology.

Materials and methods

A highly oriented pyrolytic graphite (HOPG) ($d_{002} = 0.335$, $L = 500$ nm) was used for synthesis of graphite intercalated with cobalt. Intercalated graphite (IG) specimens were obtained by two-stage method with usage of C_8K as precursor [29]. At the first stage, the graphite intercalated with potassium according to equation $\text{C} + \text{K} \rightarrow \text{C}_8\text{K}$ was obtained by standard gas-phase method. At the second stage, cobalt chloride in the interlayer space of graphite was reduced to cobalt by the following scheme: $\text{C}_8\text{K} + \text{MeCl}_x \rightarrow \text{C} - \text{Me} + \text{KCl}$. Metal chloride reduction reaction was carried out in the medium of tetrahydrofuran. The structure and phase composition of obtained IG specimens were investigated using DRON-4-07 automated X-ray diffractometer in filter NiK_α radiation (wavelength is 0.165791 nm).

Figure 1 presents the X-ray diffraction pattern for synthesized GIC. As one can see, the diffraction pattern contains system of peaks, which correspond

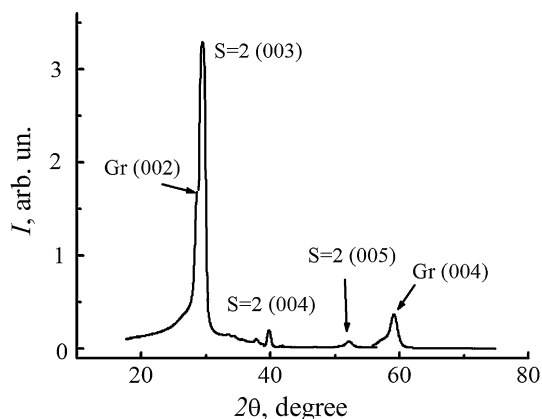


Figure 1 X-ray diffraction pattern for synthesized GIC.

to reflections from cobalt layers and are placed between layers of graphite. The analysis of X-ray diffraction data has showed that obtained specimens are intercalated compounds of second stage with such parameters: the stage number (S ; the number of graphite layers between two layers of intercalate) equals to 2; the identity parameter (I_s ; the distance between the subsequent intercalate layers separated by S graphite layers) equals to 0.975 nm; the distance (d_s ; the distance between two graphite layers, which contain an intercalate layer) equals to 0.305 nm. A more detailed description of IG structure is presented in [29].

The measurements of resistance along graphite planes and resistance in transverse magnetic field were taken with standard four-probe method in the temperature range of (1.6–293) K and magnetic fields up to 5 T. Measurement error does not exceed 0.05%. The magnetoresistance was calculated using the equation: $\frac{\Delta\rho}{\rho} = \frac{\rho(B) - \rho_0}{\rho_0}$, where $\rho(B)$ is the resistivity in magnetic field of induction B and ρ_0 is the resistivity in zero magnetic field.

Results and discussion

Figure 2 presents the typical temperature dependence of resistivity ($\rho_a(T)$) along graphite planes for obtained GIC. For comparison the $\rho_a(T)$ dependence for HOPG is presented too. As one can see, the character of temperature dependence $\rho_a(T)$ for GIC is essentially different from such dependence for HOPG. So, the HOPG resistivity at low temperatures practically does not change with temperature. With further temperature increasing the resistivity slightly

decreases ($\rho_{a4.2}/\rho_{a293} \sim 1.75$). This is due to increasing of charge carriers concentration and weak decrease in charge mobility in graphite with increasing of temperature in conditions of preferred temperature independence crystallite boundary charge carriers scattering. Unlike to HOPG for GIC the increasing of resistivity with temperature is observed ($\rho_{a4.2}/\rho_{a293} \sim 0.8$). Such resistivity temperature dependence $\rho_a(T)$ is typical for GIC based on HOPG and described in a large number of work [30–33]. It is known that during the intercalation process there is a transfer of charge from intercalate molecules to graphite layers. The increasing in the concentration of charge carriers in graphite layers after intercalation process is the cause of GIC conductivity growth. Thus, the character of temperature dependence of resistivity for obtained IG specimens is an additional argument in favor that the intercalation occurred. Note, that at low temperature the minimum in dependence of $\rho_a(T)$ is observed. Such abnormal minimum in $\rho_a(T)$ dependence was observed in several studies of acceptor-type GICs based on the fine crystalline anisotropic graphite and graphite fibers [34, 35]. These anomalies are explained by manifestation of weak localization of charge carriers and interaction effects. However, for GICs based on HOPG such anomalies in the temperature dependence of resistivity have not been previously revealed.

Figure 3 presents the dependences of magnetoresistance on magnetic field ($\Delta\rho/\rho(B)$) for GIC in the temperature range of (1.6–50) K. For comparison $\Delta\rho/\rho(B)$ dependence for HOPG is presented too.

As one can see, the character of $\Delta\rho/\rho(B)$ dependence for HOPG is typical for graphite with structure of natural monocrystalline graphite (Fig. 3a). Magnetoresistance is symmetric relatively to magnetic field direction and proportional to square of magnetic field. With temperature decreasing the magnetoresistance increases. This effect is explained by increasing of charge carrier's mobility with decrease in temperature.

The cobalt intercalation into graphite results in significant differences in $\Delta\rho/\rho(B)$ dependences for GIC in comparison with HOPG (Figs. 3b–f). The magnetoresistance for IGC is positive as for HOPG. The value of magnetoresistance is large enough, unlike to classical GICs with alkali metals or salts, where the introduction of intercalate into graphite is accompanied by a significant (almost zero) decrease

Figure 2 $\rho_a(T)$ dependences for GIC (a) and HOPG (b).

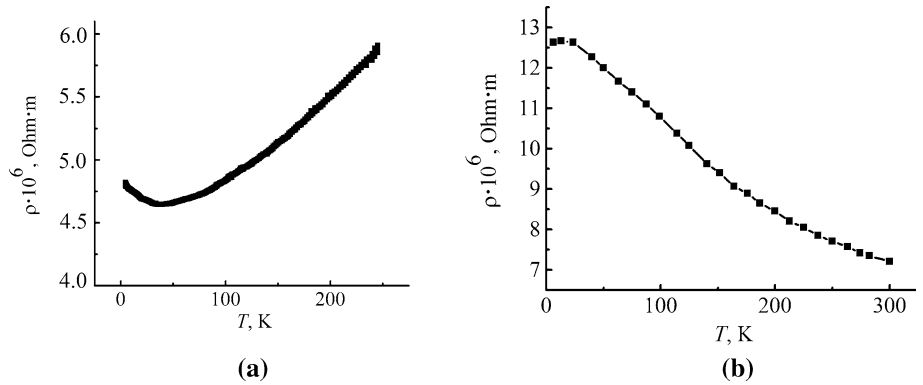
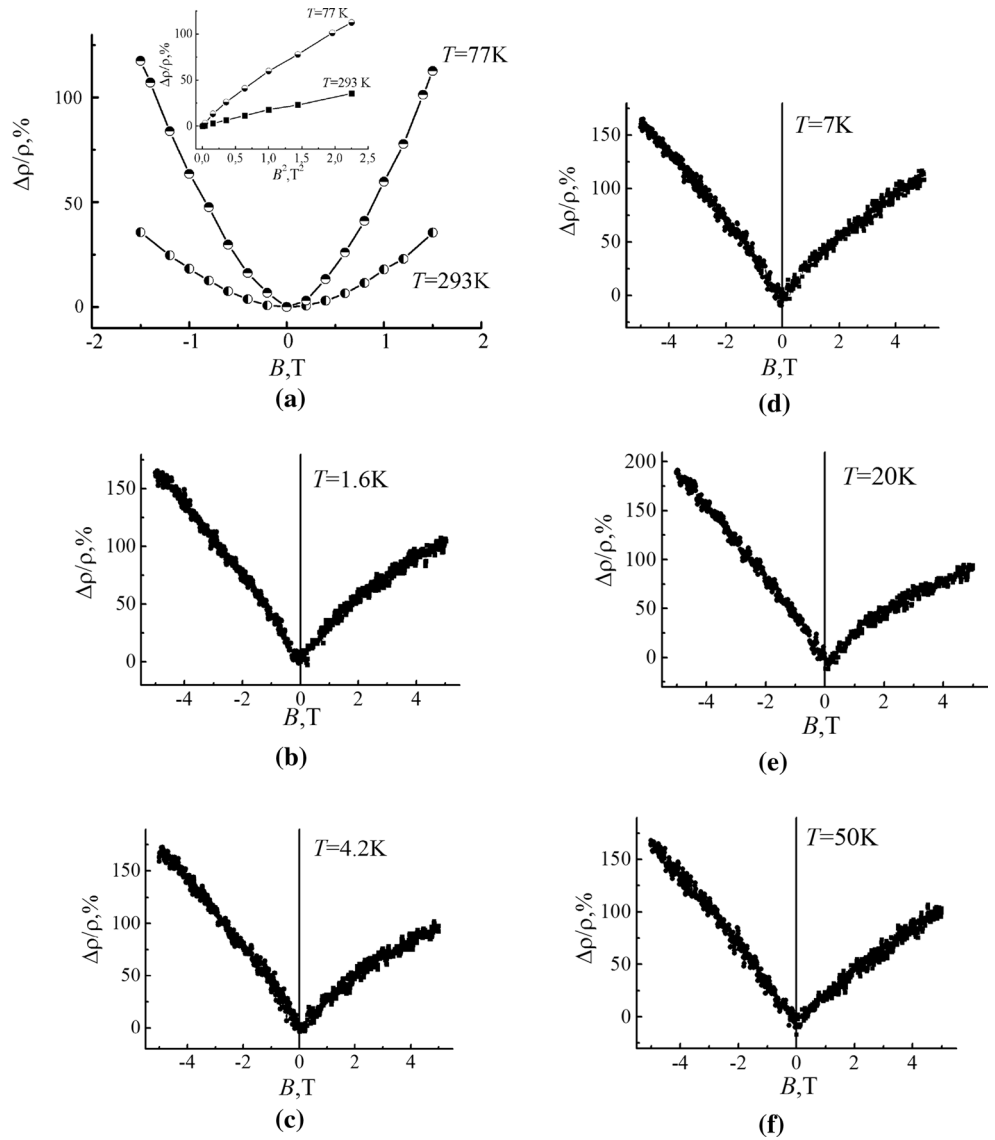


Figure 3 $\Delta\rho/\rho(B)$ dependences for HOPG (a) and GIC at different temperatures: 1.6 K (b), 4.2 K (c), 7 K (d), 20 K (e) and 50 K (f).



in magnetoresistance. But the most interesting is that for GIC there is asymmetric relatively to magnetic field direction magnetoresistance at all studied

temperatures. This effect was first found by us in the works [36–38]. In [38] this effect has been detail analyzed and explained in the terms of Segal model.

Segal et al. proposed a model [39], in which an anomalous dependence of magnetoresistance on the magnetic field direction, that is observed for multi-layer films Co/Pd and Co/Pt [40], epitaxial structures Ga, Mn, As [41] and thin nickel films [39], is explained by the gradual variation in magnetization and Hall resistivity along the specimen. Necessary conditions for the emergence of an asymmetric magnetoresistance according to the Segal model are: the presence of even insignificant heterogeneity in the structure of material containing the magnetic and nonmagnetic phases (1); the heterogeneity of the samples' magnetization in different directions (2) and a variation of Hall voltage along the specimen (3). The detailed studies demonstrate that GIC satisfies to all requirements of Segal model. So, the electron microscopy has shown [29] that GIC is a heterogeneous system, consisting of the graphite matrix, in which the clusters of intercalated graphite are distributed. The size of fragments of nonintercalated graphite is from 5 up to 20 nm. Nanoparticles of GIC with cobalt are situated in a graphite matrix quite uniformly, although they vary considerably in thickness. The size of intercalated graphite parts is in interval from 2 to 20 nm. The study of magnetic properties has shown that GIC is layered ferromagnetic system with high magnetic anisotropy [29]. The value of magnetization along the graphite plane (along the specimen) is almost an order of magnitude smaller than magnetization along the C axis. Finally, it was shown in [36, 38] that formation of ferro- (antiferro-)magnetic clusters in graphite matrix leads to the appearance in GIC of the extraordinary Hall effect caused by the spin-orbit interaction between the electrons and carriers in the intercalate.

On the basis of Segal model, an algorithm was proposed, which allows to split the experimental dependence of magnetoresistance on magnetic field into the square and linear parts [38]. Let us apply this algorithm to analyze the magnetoresistance field dependencies for obtained GIC.

According to [38], the resistivity dependence on magnetic field can be presented as

$$\rho(B) = \rho_e(B) + \rho_n(B), \quad (1)$$

where $\rho_e(B)$ is an even function of the magnetic field, and $\rho_n(B)$ is odd one and is proportional to the transverse Hall voltage. Second term in (1) occurs in the presence of transverse voltage due to varying of the size of magnetic clusters and value of local Hall

coefficient along the specimen. This term can be presented as $\rho_n(B) = \alpha B$, where α is some coefficient. Thus, an Eq. (1) can be rewritten for positive and negative directions of magnetic field as following

$$\begin{aligned} \rho(B) &= \rho_e(B) + \beta B \\ \rho(-B) &= \rho_e(-B) - \beta B, \end{aligned} \quad (2)$$

where $\rho_e(B) = \rho_e(-B)$.

Figure 4 presents the calculated even relatively magnetic field direction magnetoresistance term $\frac{\rho_e(B) - \rho_0}{\rho_0} \cdot 100\% \equiv \left(\frac{\Delta\rho}{\rho}\right)_e = f(B)$ at different temperatures. Thus, a consideration of the linear relatively magnetic field component of magnetoresistance completely removes asymmetry of magnetoresistance for IGC.

As one can see, the values of magnetoresistance in the temperature range of (1.6–50) K are almost equal, and the field dependence of magnetoresistance is linear relatively magnetic induction starting approximately from the magnetic field $B \sim 1.2$ T.

The fragments of magnetoresistance depending on magnetic field with account of linear term for GIC at temperatures of 1.6, 4.2 and 20 K are presented on Fig. 5. As one can see, the linear dependence of magnetoresistance on magnetic field is really observed for the studied GIC in the magnetic field over 1.2 T at temperature $T = 1.6$ K and over 1 T at temperature $T \geq 4.2$ K.

Let us consider the possible mechanisms of such large linear magnetoresistance for IGC. According to conventional theory the magnetoresistance $\Delta\rho$

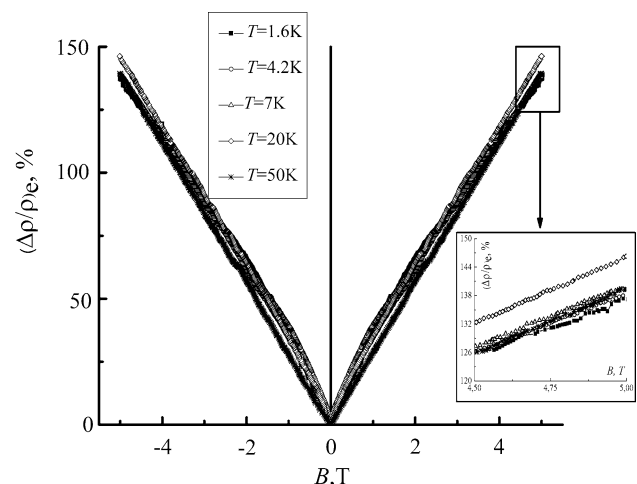


Figure 4 $\left(\frac{\Delta\rho}{\rho}\right)_e = f(B)$ dependences for GIC at different temperatures.

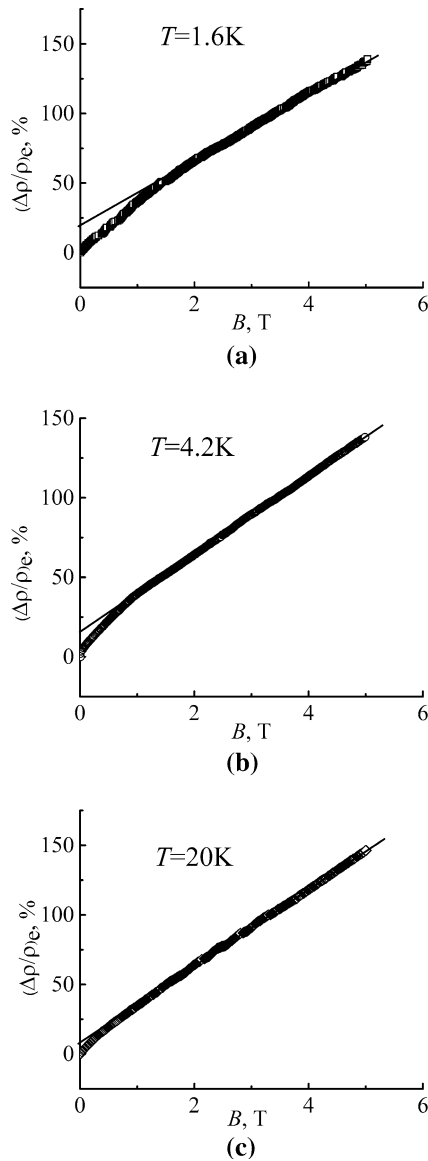


Figure 5 Fragments of $\left(\frac{\Delta\rho}{\rho}\right)_e = f(B)$ dependence at different temperatures: 1.6 K (a), 4.2 K (b) and 20 K (c).

$(\Delta\rho = \rho(B) - \rho(0))$ in a metal with nonequal densities of electrons and holes behaves as

$$\Delta\rho \propto \begin{cases} \rho_0 \cdot (\omega_c\tau)^2, & \omega_c\tau \ll 1 \\ \rho_0, & \omega_c\tau \gg 1 \end{cases} \quad (3)$$

where $\omega_c = \frac{eB}{m^*}$ is the Larmor frequency, m^* is the cyclotron mass and τ is the collision time. So, in weak magnetic fields ($\omega_c\tau \ll 1$) $\Delta\rho$ quadratically depends on the magnetic field, and with increasing magnetic field and reaching the condition $\omega_c\tau \gg 1$ value of $\Delta\rho$ reaches saturation. Exception is material with an open Fermi surface or compensated homogeneous

semiconductor, where magnetoresistance increases with increasing magnetic field without saturation, but proportionally to B^2 . However, a significant ($\sim 200\text{--}1000\%$) linear magnetoresistance has been revealed for a number of narrow-gap disordered semiconductors at extremely small magnetic fields. Moreover, the magnetoresistance' saturation has not been observed at high magnetic fields. In particular, this effect was observed for silver chalcogenides, MnAs-GaAs, layered structure PrFeAsO and graphene [1–3, 5, 6, 42].

Now, there are two approaches for explanation of this phenomenon. Within the terms of classical approaches the causes of linear magnetoresistance, which is not saturable at high magnetic field, are (1) the macroscopic fluctuations of carrier mobility in the clusters with significantly different conductivity, (2) the relatively large pores and (3) the magnetic breakdown. Numerical calculations shown that the spatial fluctuations of charge mobility can change the conductivity tensor that causes a linear magnetoresistance. This mechanism probably can be used to explain the effect of linear magnetoresistance in granular systems, which are composed of pellets with substantially different conductivity (for example, metal clusters in dielectric matrix), that provides the spatial changes in conductivity.

Another approach to explain the linear magnetoresistance was proposed by Abrikosov [11, 43, 44]. Abrikosov has received the following dependence of conductivity on the magnetic field

$$\frac{\sigma_0}{\sigma} = \frac{\rho}{\rho_0} = \frac{N_i B}{\pi n^2 e} \propto B, \quad (4)$$

where σ_0 and ρ_0 are the conductivity and resistivity in zero magnetic field, n is the electron density, N_i is the density of scattering centers. As one can see, the magnetoresistance is linear at a relatively small magnetic fields, it is positive, does not reach the saturation and does not depend on temperature. This model can be extended for doped layered structures with metallic conductivity and graphite-like (quasi-linear) energy spectrum, if there are a weak interlayer interaction and high anisotropy of effective mass [43]. For such structures, the magnetoresistance is also linearly increases with magnetic field increasing

$$\frac{\rho_{xx}}{\rho_0} = \frac{N_i B}{\pi n_0^2 e} \frac{\sinh(1/\theta)}{\cosh(m/\theta) + \cosh(m/\theta)} \propto B, \quad (5)$$

where $\theta = T/t$, $m = \mu/t$, $2t$ is the band width and μ is the level of the chemical potential.

Let us consider the possibility of implementing each of the two proposed linear magnetoresistance mechanisms for GIC with cobalt. But to assess the possibility of using mechanisms of linear magnetoresistance, the additional studies of obtained GIC were necessary. So, to determine the charge carriers concentration and Fermi energy for GIC the Hall coefficient temperature dependence has been measured.

Figure 6 presents the Hall coefficient temperature dependence ($R_H(T)$) for GIC at $B = 5$ T. As one can see, the Hall coefficient is positive, that indicates on the hole conductivity in GIC, and it is independent on temperature, that is typical for low-stage GIC. The bulk charge concentration $n_v = 1.56 \times 10^{24} \text{ 1/m}^3$ was determined from experimental data according to equation $n_v = 1/eR_H$.

Let us estimate the value of additional charge transferred from intercalate molecules to graphite layer (i.e., accommodation coefficient f), and also the Fermi energy E_F in the terms of ordinary 2D model of electron structure of GICs (the model of “metallic sandwich” [45–47]). Within this model, the GIC electronic structure is considered as the sequence of bands with low and high free charge carrier density along C axis. One of these bands corresponds to pure 3D graphite, and another corresponds to 2D “metallic sandwich” consisted of intercalate layer and two neighboring graphite layers. Bulk charge carrier concentration n_v in the “metallic sandwich” is determined mainly by the number of transferred charge from intercalate layers to graphite layer

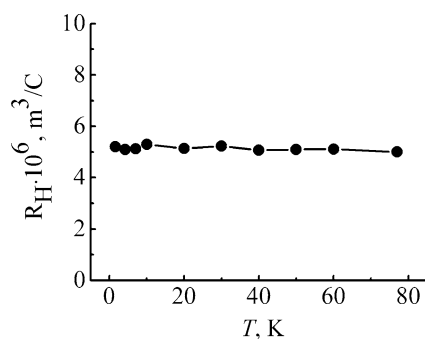


Figure 6 $R_H(T)$ dependence for GIC at $B = 5$ T.

$$n_v = \frac{N_c}{Sp^*} f \frac{d_{002}}{d_s}, \quad (6)$$

where N_c is the concentration of carbon atoms, which is much higher than own concentration of electrons and holes in the HOPG, f is the accommodation coefficient, S is the stage number, p^* is the stoichiometric index in GIC formula. The Fermi energy E_F associated with accommodation coefficient by the following relationship

$$E_F = \gamma_0 \left(\frac{\sqrt{3}\pi f}{p^* S} \right)^{\frac{1}{2}}, \quad (7)$$

where $\gamma_0 = 3.2$ eV is the interaction of neighboring atoms in a graphite layer. The estimated values of f and E_F are $f = 0.0009$ and $E_F = 0.04$ eV, respectively. Thus, the redistribution of charge between the layers of graphite and intercalate, which occurs during intercalation process, leads to the shift of E_F into valence band and independence of carriers concentration on the temperature in a wide range. However, note that the obtained values of the concentration of charge carriers, the charge values transferred from the intercalation molecules to the graphite layers and, accordingly, the Fermi level shift for the investigated compound is smaller than, for example, for compounds of the acceptor type with halogens or halides [48]. Another important parameter for assessing the application of a mechanism of linear magnetoresistance is the value of the mobility of charge carriers μ . To estimate the value of μ and its temperature dependence $\mu(T)$, we can use the experimental temperature dependence of the specific resistance $\rho(T)$ (Fig. 2a). Since, as shown above, the concentration of charge carriers in the GIC does not depend on temperature, the growth of the specific resistance of the GIC occurs only due to a slight decrease in the mobility of the charge carriers with temperature rise in accordance with $\frac{1}{\rho} = en_v\mu$. The estimation of the temperature dependence of mobility in the approximation, that the specific resistance of the GIC is linearly dependent on temperature leads to a correlation $\mu(T) = \mu_0 + k_\mu \Delta T$, where μ_0 is the charge carriers mobility at the highest temperature of measurement $T = 250$ K, $\mu_0 = 0.529 \text{ m}^2/\text{V s}$, k_μ is the temperature ratio of mobility, $k_\mu = -6.32 \times 10^{-4} \text{ m}^2/\text{V s K}$. Note that the low-temperature abnormal dependence $\rho(T)$ is not taken into account here. Thus, within such an

approximation, mobility at $T = 1.6$ K $\mu_0 = 0.692$ m²/V s, and at $T = 20$ K, $\mu_0 = 0.681$ m²/V s.

Let us estimate the use of various theories of linear magnetoresistance to its explanation in GIC with cobalt. In the terms of classical theory of Parish and Littlewood the macroscopic fluctuations of carrier mobility in the clusters with significantly different conductivity are decisive. However, for GIC such mechanism for explanation of linear magnetoresistance is questionable. First, despite the fact that GIC with cobalt is heterogeneous system, the carrier's mobility in the clusters of HOPG and GIC does not differ significantly. As it is known, charge carrier mobility μ for HOPG is ~ 1.6 m²/V s. For GIC with cobalt the value of μ is $\sim (0.5\text{--}0.7)$ m²/V s as shown above. Thus, the values of mobility of the clusters of HOPG and GIC are different, but their difference is not so significant. Second, the model of classical linear magnetoresistance demonstrates that magnetic field B_0 , at which there is a transition from linear to quadratic dependence of magnetoresistance on magnetic field, is proportional to $1/\mu$. Therefore, given that the mobility of carriers in HOPG and GIC clusters slightly decreases with increasing temperature, one can expect that the transition field B_0 will slightly increase with temperature increasing. However, as one can see from Fig. 5, the transition field B_0 somewhat decreases with temperature rise. The ratio of the experimental values of the transition fields to the linear dependence of the magnetoresistance $B_{01.6}$ and B_{020} at temperatures 1.6 and 20 K is ~ 1.2 , while the ratio of the calculated values of the transition fields at the same temperatures is ~ 0.984 . Finally, the classical model assumes that linear magnetoresistance increases due to carrier mobility fluctuations with increasing temperature that is not observed for GIC.

The necessary conditions for the realization of quantum Abrikosov linear magnetoresistance mechanism are the presence in the material of the layered structure with the weak interaction between layers and quasi-linear dispersion law. Obviously, these conditions are realized for any low stage of GICs. So, HOPG is a layered material in which the covalent bonds in the graphite layer are almost ten times larger than weak bonds between the graphite layers. For GICs, this difference increases and, moreover, the graphite layers on both sides of intercalate layer do not interact with each other. According to the electronic structure model for acceptor GIC [45–47], there

is a linear dispersion law for a first-stage compound and quasi-linear dispersion law for a second-stage compound.

Quantum linear magnetoresistance is fulfilled under the conditions $\omega_c \hbar \gg k_B T$ and $\omega_c \hbar > E_F$ [11, 12], where ω_c is the cyclotron frequency, $\omega_c = eB/m^*$ (m^* is the effective charge carrier mass, $m^* = 0.05 m_e$ (m_e is the free electron mass) according to [49]). Let's evaluate the value of the magnetic field, above which it is possible to observe a quantum linear magnetoresistance at different temperatures. The calculated values of the magnetic field under which the condition for observing quantum linear magnetoresistance is fulfilled are $B \gg 0.04$ T at $T = 1.6$ K, $B \gg 0.22$ T at $T = 4.2$ K, $B \gg 0.3$ T at $T = 7$ K and $B \gg 0.8$ T at $T = 20$ K. Thus, the magnetic fields in which the transition to a linear magnetoresistance is experimentally observed in GIC with cobalt, satisfy the condition $\omega_c \hbar \gg k_B T$. In this case, the energy $\hbar \omega_c$ and E_F have comparable values. In order for the condition $\omega_c \hbar > E_F$ to be fulfilled in full, the effective mass of charge carriers should be not more $0.01 m_e$. However, it is known, the intercalation of graphite with halogens and halides leads to an increase in several times the effective mass of charge carriers and to a significant displacement of the Fermi level in the valence band depth (up to 1 eV) for compounds of low stages. This makes it impossible to observe a quantum linear magnetoresistance in such GICs, despite the layered structure and the weak interaction between the layers of graphite, as well as the linear dispersion law for compounds of low stages.

Conclusions

Experimental studies of magnetoresistance as well as Hall coefficient and electrical resistivity are carried out for graphite intercalated with cobalt. It is revealed that for based on HOPG intercalated compounds with cobalt unusual dependence of magnetoresistance from magnetic field is observed, namely:

1. The magnetoresistance is asymmetric relative to magnetic field. This effect is due to heterogeneity of GIC structure that is result in variation of Hall voltage along the GIC specimen. The account of a linear relative magnetic field magnetoresistance component in the terms of Segal model completely removes asymmetry of magnetoresistance for graphite intercalated with cobalt;

2. The magnetoresistance is linear relative to magnetic field, does not show any signs of saturation with increasing magnetic field up to 5 T and is independent from temperature. The carried out calculations showed that for graphite intercalated with cobalt the conditions for achieving of quantum limit are fulfilled at magnetic field ~ 1 T and temperature range up to 20 K. So, one can assume that the nature of the observed linear magnetoresistance is associated with the Abrikosov mechanism.

Authors Contributions

IB, YP, LM and UR conceived and designed the experiments. IM, VT, TL and OP performed the experiments. YP, LM and IO analyzed the data. IB, IO, TL, IO contributed in the drafting and revision of the manuscript. LM, YP, IO and UR supervised the work and finalized the manuscript. All authors read and approved the final manuscript.

Compliance with ethical standards

Conflict of interest The authors declare that they have no conflict of interest.

References

- [1] Xu R, Husmann A, Rosenbaum TF, Saboungi ML, Enderby JE, Littlewood PB (1997) Large magnetoresistance in non-magnetic silver chalcogenides. *Nature* 390:57–60
- [2] Lee M, Rosenbaum T, Saboungi M, Schnyders H (2002) Band-gap tuning and linear magnetoresistance in the silver chalcogenides. *Phys Rev Lett* 88:066602–066604
- [3] Kreuzbruck M, Lembke G, Mogwitz B, Korte C, Janek J (2009) Linear magnetoresistance in $\text{Ag}_2 + \delta\text{Se}$ thin films. *Phys Rev B* 79:035204–035205
- [4] Branforda WR, Husmann A, Solin SA, Clowes SK, Zhang T, Bugoslavsky YV, Cohen LF (2005) Geometric manipulation of the high-field linear magnetoresistance in InSb epilayers on GaAs (001). *Appl Phys Lett* 86:202116-1–202116-3. doi:10.1063/1.1923755
- [5] Johnson H, Bennett S, Barua R, Lewis L, Heiman D (2010) Universal properties of linear magnetoresistance in strongly disordered MnAs-GaAs composite semi-conductors. *Phys Rev B* 82(6):085202–085204
- [6] Bhoi D, Mandal P, Choudhury P, Pandya S, Ganesan V (2011) Quantum magnetoresistance of the PrFeAsO oxypnictide. *Appl Phys Lett* 98(17):172105-1–172105-3
- [7] Wang XL, Du Y, Dou SX, Zhang C (2012) Room temperature giant and linear magnetoresistance in topological insulator Bi_2Te_3 nanosheets. *Phys Rev Lett* 108(26):266806-1–266806-5
- [8] Yan Y, Wang X, Yu DP, Liao ZM (2013) Large magnetoresistance in high mobility topological insulator Bi_2Se_3 . *Appl Phys Lett* 103(2):033106-1–033106-4
- [9] Singh S, Gopal RK, Sarkar J, Mitra C (2015) Quantum and classical contributions to linear magnetoresistance in topological insulator thin films. In International Conference on Condensed Matter and Applied Physics (ICC 2015) AIP Conf. Proc. 1728 pp. 020557-1–020557-4
- [10] Hu J, Parish MM, Rosenbaum TF (2007) Nonsaturating magnetoresistance of inhomogeneous conductors: comparison of experiment and simulation. *Phys Rev B* 75(21):214203-1–214203-9
- [11] Abrikosov A (1998) Quantum magnetoresistance. *Phys Rev B* 58(5):2788–2794
- [12] Friedman AL, Tedesco JL, Campbell PM, Culbertson JC, Aifer E, Perkins FK, Myers-Ward RL, Hite JK et al (2010) Quantum linear magnetoresistance in multilayer epitaxial graphene. *Nano Lett* 10:3962–3965
- [13] Singh RS, Wang X, Chen W, Wee ATS (2012) Large room-temperature quantum linear magnetoresistance in multilayered epitaxial graphene: evidence for two-dimensional magnetotransport. *Appl Phys Lett* 101(18):183105-1–183105-5
- [14] Gryglas-Borysiewicz M, Jouault B, Tworzydło J, Lewinska S, Strupinski W, Baranowski JM (2009) Transport properties of disordered graphene layers. *Acta Phys Polonica A* 116(5):838–840
- [15] Kisslinger F, Ott C, Heide C, Kampert E, Butz B, Spiecker E, Shallcross S, Weber HB (2015) Linear magnetoresistance in mosaic-like bilayer graphene. *Nat Phys Lett* 11:650–653
- [16] Zhang X, Xue QZ, Zhu DD (2004) Positive and negative linear magnetoresistance of graphite. *Phys Lett A* 320:471–477
- [17] Chacon-Torres JC, Wirtz L, Pichler T (2014) Raman spectroscopy of graphite intercalation compounds: charge transfer, strain, and electron-phonon coupling in graphene layers. *Phys St Sol B* 251(11):2337–2355
- [18] Shuvayev A, Helmer B, Lyubeznova T, Mirmilstein A, Kvacheva L, Novikov Yu, Volpin M (1989) EXAFS study of graphite intercalation compounds with transition metals (Fe, Ni). *J Phys* 50:1145–1151

- [19] Touzain F, N'Guessan G, Bonnin D, Kaiser P, Chouteau G (1996) Electrochemically reduced cobalt-graphite intercalation compound. *Synth Met* 79(3):241–251
- [20] Korolovych VF, Nedyak SP, Moroz KO, Prylutsky YuI, Scharff P, Ritter U (2013) Compressibility of water containing single-walled carbon nanotubes. *Fullerenes, Nanotubes, Carbon Nanostruct* 21(1):24–30
- [21] Korolovych VF, Bulavin LA, Prylutsky YuI, Khrapatiy SV, Tsierkezos N, Ritter U (2014) Influence of single-walled carbon nanotubes on the thermal expansion of water. *Int J Thermophys* 35(1):19–31
- [22] Buchelnikov AS, Voronin DP, Kostjukov VV, Deryabina TA, Khrapatiy SV, Prylutsky YuI, Ritter U, Evstigneev MP (2014) Complexation of aromatic drugs with single-walled carbon nanotubes. *J Nanopart Res* 16(7):2472-1–2472-14
- [23] Radchenko NV, Prylutsky YI, Shapoval LM, Sagach VF, Davydovska TL, Dmitrenko OV, Stepanenko LG, Pobigailo LS, Schütze C, Ritter U (2013) Impact of single-walled carbon nanotubes on the medullary neurons in spontaneously hypertensive rats. *Mat-Wiss U Werkstofftech* 44(2–3):171–175
- [24] Minchenko OH, Tsymbal DO, Minchenko DO, Prylutska SV, Cherepanov VV, Prylutsky YI, Tsierkezos NG (2016) Single-walled carbon nanotubes affect the expression of the *CCND2* gene in human U87 glioma cells. *Mat-Wiss U Werkstofftech* 47(2–3):180–188
- [25] Shapoval LM, Prylutska SV, Kotsyuruba AV, Dmitrenko OV, Prylutsky YuI, Sagach VF, Ritter U (2016) Single-walled carbon nanotubes modulate cardiovascular control in rats. *Mat-Wiss U Werkstofftech* 47(2–3):208–215
- [26] Mykhailenko OV, Prylutsky YuI, Matsuy DV, Strzheimchyn YM, Le Normand F, Ritter U, Scharff P (2010) Structure and thermal stability of Co- and Fe-intercalated double graphene layers. *J Comput Theor Nanosci* 7(6):996–999
- [27] Radchenko TM, Tatarenko VA, Sagalianov IYu, Prylutsky YuI, Szroeder P, Biniak S (2016) On adatomic-configuration-mediated correlation between electrotransport and electrochemical properties of graphene. *Carbon* 101:37–48
- [28] Mykhailenko OV, Prylutsky YuI, Komarov IV, Strungar AV (2017) Structure and thermal stability of Co- and Fe-intercalated double silicene layers. *Nanoscale Res Lett* 12:110-1–110-5
- [29] Matsui D, Prylutsky Yu, Matzui L, Zakharenko N, Normand F, Derory A (2010) Magnetic properties of cobalt-carbon nanocomposites. *Phys St Sol C* 7:1264–1268
- [30] Matzui L, Vovchenko L, Dvorkina I (1995) Transport properties of acceptor graphite intercalated compounds. *Ukr J Phys* 40(1–2):107–111
- [31] Sugihara K, Matsubara K, Suzuki S, Suzuki M (1998) Theory of the a- and c- axis resistivity and magnetoresistance in MoCl_5 graphite intercalation compounds. *J Phys Soc Jap* 67(12):4169–4177
- [32] Matsubara K, Sugihara K, Suzuki I, Suzuki M (1999) A- and c-axis resistivity and magnetoresistance in MoCl_5 graphite intercalation compounds. *J Phys Cond Matt* 11:3149–3160
- [33] Matsui D, Ovsyenko I, Lazarenko O, Prylutsky Yu, Matsui V (2011) Abnormal electron transport in graphite intercalation compounds with iron. *Mol Cryst Liq Cryst* 535(1):64–73
- [34] Piraux L, Bayot V, Dresselhaus M (1992) Influence of magnetic fields on the two-dimensional electron transport in weakly disordered fluorine-intercalated graphite fibers. *Phys Rev B* 45(24):14315–14320
- [35] Matzui L, Vovchenko L, Dvorkina I (1994) Low-temperature thermopower in disordered graphite intercalated with SbCl_5 . *Low Temp Phys* 20(5):463–468
- [36] Matsui D, Prylutsky Yu, Matzui L, Normand F, Ritter U, Scharff P (2008) Transverse and longitudinal magnetoresistance in graphite intercalated by Co. *Physica E* 40(7):2630–2634
- [37] Grechnev GE, Lyogenkaya AA, Kolesnichenko YA, Prylutsky YI, Hayn R (2014) Electronic structure and magnetic properties of graphite intercalated with 3d-metals. *Low Temp Phys* 40(5):580–584
- [38] Tkachuk V, Ovsyenko I, Matzui L, Len T, Prylutsky Yu, Brusylovets O, Berkutov I, Mirzoiev I et al (2016) Asymmetric magnetoresistance in the graphite intercalation compounds with cobalt. *Mol Cryst Liq Cryst* 639(1):137–150
- [39] Segal O, Shaya O, Karpovski M, Gerber A (2009) Asymmetric field dependence of magnetoresistance in magnetic films. *Phys Rev B* 79(14):144434–144436
- [40] Cheng X, Urazhdin S, Tchernyshyov O, Chien C, Nikitenko V, Shapiro A, Shull R (2004) Antisymmetric magnetoresistance in magnetic multilayers with perpendicular anisotropy. *Phys Rev Lett* 94:017203–017204
- [41] Xiang G, Holleitner A, Sheu B, Mendoza F, Maksimov O, Stone M, Schiffer P, Awschalom D, Samarth N (2005) Magnetoresistance anomalies in (Ga, Mn)As epilayers with perpendicular magnetic anisotropy. *Phys Rev B* 71(24):241307-1–241307-4
- [42] Wang X-L, Dou SX, Zhang C (2010) Zero-gap materials for future spintronics, electronics and optics. *NPG Asia Mater* 2(1):31–38
- [43] Abrikosov AA (2000) Quantum linear magnetoresistance. *Europhys Lett* 49(6):789–793
- [44] Abrikosov A (1999) Quantum magnetoresistance of layered semimetals. *Phys Rev B* 60(6):4231–4234

- [45] Blinowski J, Rigaux C, Nguyen H (1980) Band structure model and dynamical dielectric function in lowest stages of graphite acceptor compounds. *J Phys* 41(1):47–58
- [46] Blinowski J, Rigaux C (1980) Electronic properties of graphite intercalation compounds. *J Phys* 41(7):667–674
- [47] Hau NH, Blinowski J, Rigaux C (1981) Intervalence transitions in graphite acceptor compounds. *Synth Met* 3:99–105
- [48] Matzui LYu, Ovsienko IV, Vovchenko LL (2000) Phonon drag in GICs based on disordered graphite. *Mol Cryst Liq Cryst* 340(1):319–324
- [49] Buryakov T, Romanenko A, Anikeeva O, Okotrub A, Yudanov N, Kotosonov A (2007) Electrophysical properties of bromine-intercalated low-dimensional carbon structures. *Low Temp Phys* 33(2):268–271